

Tracking wakefulness as it fades: micro-measures of Alertness

Sridhar R. Jagannathan^{1*}, Alejandro E. Nassar¹, Barbara Jachs¹, Olga V. Pustovaya^{2,3}, Corinne A. Bareham⁴, Tristan A. Bekinschtein^{1,3}

¹ Department of Psychology, University of Cambridge, Cambridge, United Kingdom

² Department of man and animals physiology, Southern Federal University (SFU), Rostov-on-Don, Russia

³ Cognition and Brain Sciences Unit, Medical Research Council, Cambridge, United Kingdom

⁴ Department of Clinical Neurosciences, University of Cambridge, Cambridge, United Kingdom

*Corresponding author: j.sridharrajan@gmail.com

Present Address: Department of Psychology, University of Cambridge, Downing Street, Cambridge CB2 3EB, United Kingdom.

Abstract

A major problem in psychology and physiology experiments is drowsiness, around a third of participants show decreased wakefulness despite being instructed to stay alert. In non-visual experiments participants keep their eyes closed throughout the task, thus promoting the occurrence of such periods of varying alertness. These wakefulness changes contribute to systematic noise in data and measures of interest. To account for this omnipresent problem in data acquisition we defined criteria and code to allow researchers to detect and control for varying alertness in electroencephalography (EEG) experiments. We first revise a visual-scoring method developed for detection and characterization of the sleep-onset process, and adapt the same for detection of alertness levels. Further, we show the major issues preventing the practical use of this method, and overcome these issues by developing an automated method based on frequency and sleep graphoelements, which is capable of detecting micro variations in alertness. The validity of the automated method was verified by training and testing the algorithm using a dataset where participants are known to fall asleep. Further, we tested generalizability with independent validation on another dataset. The methods developed constitute a unique tool to assess micro variations in levels of alertness and control trial-by-trial retrospectively or prospectively in every experiment performed with EEG in cognitive neuroscience.

Keywords:

Alertness, micro-measures, Electroencephalography, drowsiness

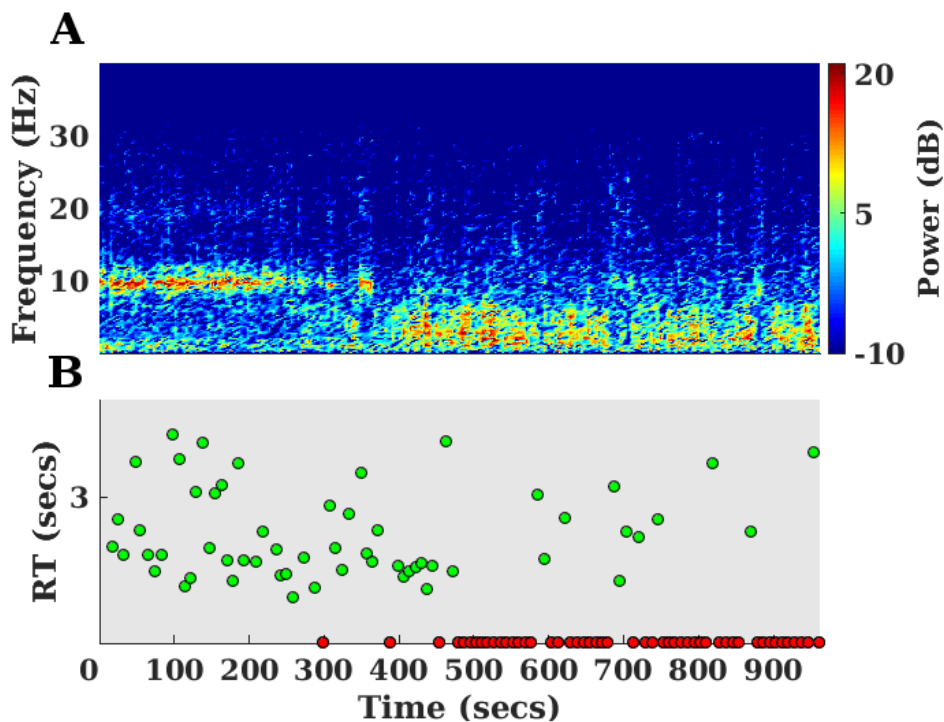
36 **1. Introduction**

37 Electroencephalography (EEG) has played a pivotal role in the non-invasive study of brain
38 function (Niedermeyer and Silva, 2004). Typically in an EEG experiment the
39 electrophysiological activity of the brain is recorded from the scalp of the participant while they
40 are performing a cognitive task or under task-free conditions (resting state). In several task-
41 based experiments, typically in the auditory or tactile domain, the participant performs the task
42 in eyes-closed settings. Previous studies have shown that such eyes closed settings can create
43 periods of momentary lapses of alertness (Barry et al., 2007). These periods are usually
44 attributed to variable and long inter-trial intervals. The prevalence of this problem can be
45 attested by studies mining large databases showing that about a third of the participants
46 momentarily fall asleep in resting state conditions (Tagliazucchi and Laufs, 2014). Further, task
47 free settings such as mind wandering or simple non-active instructions can also lead to
48 drowsiness and sleep (Goupil and Bekinschtein, 2012).

49 The above mentioned variations in alertness can usually be detected using variability in
50 reaction times (Ogilvie, 2001). However in most of the EEG experiments such lapses are ignored
51 and data confounded with drowsiness (or low alertness) are used for studying brain functions
52 like attention and cognition. However, attention and many other cognitive sub-processes are
53 known to be directly modulated by lack of alertness in normal (Bareham et al., 2014; Chennu
54 and Bekinschtein, 2012) as well as clinical populations (Dobler et al., 2005). Hence, fluctuations
55 in alertness need to be measured by the researchers, to include or exclude trials of low/high
56 alertness to adequately test predefined hypotheses. This argument is illustrated with an
57 experiment in Figure 1.

58 Figure 1(B) shows a typical EEG experiment where the participant responds to auditory stimuli
59 while having their eyes closed. In the beginning of the experiment the participant responds to
60 the stimuli in a reliable manner (green dots) by less variation in reaction times. As time
61 progresses the reaction times become more variable and the participant intermittently fails to
62 respond (red dots). This variation is also captured in the frequency profile of the EEG (occipital
63 sites) during the pre-trial periods of the task as depicted in Figure 1(A). When the participant
64 responds reliably, the frequency profile shows clear majority of power in the alpha range (8-12
65 Hz) and as they become drowsy the power in the alpha disappears and low frequency power in
66 the theta range (6-8 Hz) starts to increase. Thus the frequency profile preceding the trial often
67 predicts the variability in the responses. In other words, such spectral changes can be used to
68 detect the momentary lapses in alertness that causes variability in the reaction times.

69 The typical techniques that are used to clean or remove the data from such drowsiness
70 contaminated episodes would be to score the above mentioned pre-trial periods using
71 traditional sleep scoring techniques (Berry et al., 2012). These scoring techniques depend on
72 the frequency profiles described earlier. However they face multiple problems. Firstly, sleep
73 scoring techniques rely on having data at least to the duration of 30 sec (Berry et al., 2012).
74 However in most cognitive experiments the pre-trial periods last at most 4-5 sec. Secondly,
75 automated methods (Tagliazucchi et al., 2012) that are validated using such sleep scoring
76 techniques classify data into wakefulness, N1, N2 etc. But such momentary lapses of alertness
77 require more fine grained scoring techniques that operate on a smaller time range with
78 different features capable of capturing micro variations in alertness levels. Finally, some
79 techniques use the simple variation in reaction times mentioned earlier to capture moments of
80 low alertness. But this suffers from the problem of longer reaction times being confounded by
81 other factors such as task difficulty (Bareham et al., 2014).



82

83 *Fig 1: Differing alertness levels indicated by frequency profile changes and reaction time*
84 *variability during an auditory experiment in a sample participant. (A) Depicts the changes in the*
85 *power level in different frequency bands in the Occipital electrodes in the pre-trial period of an*
86 *auditory experiment at different time points. (B) Reaction times at trials presented along the*
87 *different time points in the same experiment. The variability in the reaction times (B) and thus*
88 *reduction in alertness levels closely follows the change in the frequency profile (A) from alpha (8-*
89 *12 Hz) to theta (6-8 Hz)*

90 Thus the above mentioned problem of fluctuations in alertness requires a unique solution. Our
91 proposal is to tackle the problem in the following manner. Firstly, we identify these alertness
92 contaminated episodes, through the use of Hori scale (Tanaka et al., 1996) that captures the
93 micro variations in alertness. Though the prime purpose of the Hori system is to identify and
94 characterise the sleep onset process, it contains features that enable us to identify variations in
95 levels of alertness in more fine grained durations (4 sec) compared to traditional sleep scoring
96 using wakefulness, N1 and N2. Secondly, we used human scorers to identify different levels of
97 alertness using the Hori scale on a dataset where the participants are allowed to fall asleep
98 while performing the task. Thirdly, we show that despite the clarity of the Hori scale, it is
99 impractical to perform, time consuming and difficult to learn, as elucidated by the low degree of
100 agreement among human scorers. Fourthly, we produced a practical solution to this problem
101 using an automated technique (involving SVM and individual element detectors) and computed
102 performance measures by training and testing the algorithm on a dataset labelled by gold
103 standard Hori (converging ratings from multiple scorers). Finally, to estimate the reliability and
104 generalisability of our method, we tested the same in another independent dataset to show its
105 utility.

106 This paper is organized as follows. In the first section, we describe the method of using the Hori
107 scale using human scorers and provide an overview of the automated method. In the second
108 section, we evaluate and scrutinise the results of the human scorers with agreement measures
109 and motivate the use of automated algorithm using validation measures. In the final section, we

110 discuss the developments made in this paper and produce concluding remarks on the
111 usefulness of the method developed here.

112 **2. Materials and methods**

113 **2.1. Participants and datasets**

114 The first dataset (herein Dataset#1) consisted of 20 native English speakers performing a
115 semantic categorization task while falling asleep (Kouider et al., 2014). The task consisted of
116 listening to words that belong to a particular semantic category (e.g. animals or objects) and
117 classifying them accordingly using a left or right button press. Each trial consisted of an auditory
118 stimulus (spoken word: animal or object) presented binaurally with an intertrial interval of 6-9
119 sec.

120 The second dataset (herein Dataset#2) consisted of 31 participants performing an auditory
121 masking task while falling asleep (Noreika et al., 2017a). The task consisted of listening to a
122 target sound (e.g. beep) that was randomly masked by different durations of noise. Participants
123 reported if they heard the target or not using a button press. Each trial consisted of an auditory
124 stimulus (target) sometimes masked by noise, presented binaurally. The next trial was
125 presented after a pause of 8-12 sec after the response or 13-17 sec (in case of no response).

126 In both the experiments subjects were seated on a reclining chair in a dark room and were
127 permitted to fall asleep during the task. The participants were also evaluated on the basis of
128 Epworth Sleepiness scale (Johns, 1991) and only easy sleepers were recruited.

129 **2.2. EEG acquisition**

130 Dataset#1: EEG was recorded using 64 Ag/AgCl electrodes (NeuroScan labs) with Cz as
131 reference. The electrode impedances were kept below the recommended levels of the
132 manufacturer. The signal was acquired at a sampling rate of 500 Hz.

133 Dataset#2: EEG was recorded using 129 Ag/AgCl electrodes (Electrical Geodesics Inc) with Cz
134 as reference. The electrode impedances were kept below 100 K Ω . The signal was acquired at a
135 sampling rate of 500 Hz.

136 **2.3. Pre-processing**

137 EEG data was pre-processed with custom made scripts in MATLAB (MathWorks Inc. Natick, MA,
138 USA) using EEGLAB toolbox (Delorme and Makeig, 2004). The data was filtered between 1 and
139 30 Hz and was then resampled to 250 Hz. Further it was epoched from 4000ms to 0ms to the
140 onset of the stimuli. Bad channels were then detected if the activity in spectrum of the channel
141 exceeds ± 4 standard deviation of overall activity in all channels. The detected bad channels
142 were then interpolated using spherical interpolation. After which trials that exceed the
143 amplitude threshold of $\pm 250\mu\text{V}$ were removed in a semi automatic fashion. The amplitude
144 threshold was liberal as K-complexes usually exceed $\pm 150\mu\text{V}$.

145 Before proceeding to use the above datasets for scoring using the Hori scale it would be
146 pertinent for us to first introduce the Hori system of scoring and inform the readers about the
147 augmentations made in the system to suit the current purpose of measuring changes in levels of
148 alertness.

149 **2.4. Hori Scale**

150 Hori and colleagues subdivided sleep onset process into 9 different substages (Tanaka et al.,
151 1996). The first two Hori stages (1,2) correspond to wakefulness. The next six Hori stages (3-8)
152 correspond to the sleep stage N1. The last stage of Hori (9) corresponds to the beginning of N2
153 sleep (Iber et al., 2007).

154 Here we decided to augment classical Hori stages with another stage (10) that would
155 correspond to the appearance of K-complexes. The rationale behind this addition is the
156 appearance of K-complexes definitively mark the entrance to N2 sleep. While spindles can still
157 serve this purpose, their variability in duration and disagreement among human raters (Warby
158 et al., 2014) motivates the use of K-complex. The following is a brief description of the elements
159 in the hori scale based on (Ogilvie, 2001) and are shown in Figure 2.

160 **2.4.1. Alert elements**

161 **Alpha waves:**

162 Alpha waves are elements that occur in the range of 8-12 Hz during relaxed wakefulness. They
163 are more pronounced in the eyes closed condition, when the participant is transitioning from
164 alert to relaxed wakefulness (Hori 1-2). Alpha elements are usually more pronounced in EEG
165 from occipital regions.

166 Hori 1: Epoch is composed of only alpha wave trains (at least 20uV).

167 Hori 2: Alpha wave trains occupy more than 50% (but less than 100%) of the activity in the
168 epoch.

169 **2.4.2. Drowsy elements**

170 **Alpha waves:**

171 Alpha activity usually decreases when the participant transitions from relaxed wakefulness to
172 drowsy (Hori 3).

173 **Theta waves:**

174 Theta waves are elements that occur in the range of 3-8 Hz. They have relatively higher
175 amplitudes than the alpha elements and characterise the transition to N1. Theta activity is
176 usually pronounced in the central and temporal regions (Hori 5).

177 Hori 3: Alpha wave trains occupy less than 50% of the activity in the epoch.

178 Hori 4: Activity flattening without any clear element (amplitude < 20 uV).

179 Hori 5: Low voltage theta waves (ripples) with amplitude between 20 uV-50 uV.

180 **2.4.3. Grapho elements**

181 **Vertex sharp waves:**

182 Vertex waves are grapho elements that occur in the beginning of the transition to sleep (Hori 6-
183 8). Appearance of them indicates an altered state of responsiveness in the cerebral cortex
184 (Rodenbeck et al., 2006). The vertex waves can be either monophasic or biphasic. In both cases
185 there is usually a sharp negative discharge followed by a positive one. In case of biphasic waves,
186 the amplitude of the positive components should be at least 50% of the negative component and
187 at most equal to the level of the negative component.

188 Hori 6: Epoch containing only one well defined vertex sharp wave.

189 Hori 7: Epoch containing more than one vertex sharp wave.

190 **Spindles:**

191 Spindles are grapho elements that occur in the beginning of the transition to stage N2 of sleep
192 (Hori 9). They are regarded as transient patterns of EEG activity with a frequency of 12-16 Hz
193 with a minimum duration of 0.5 sec. Spindles in general should be distinguishable from the
194 background activity. The typical waxing and waning of spindle shape is vital to distinguish the
195 pattern from high alpha activity.

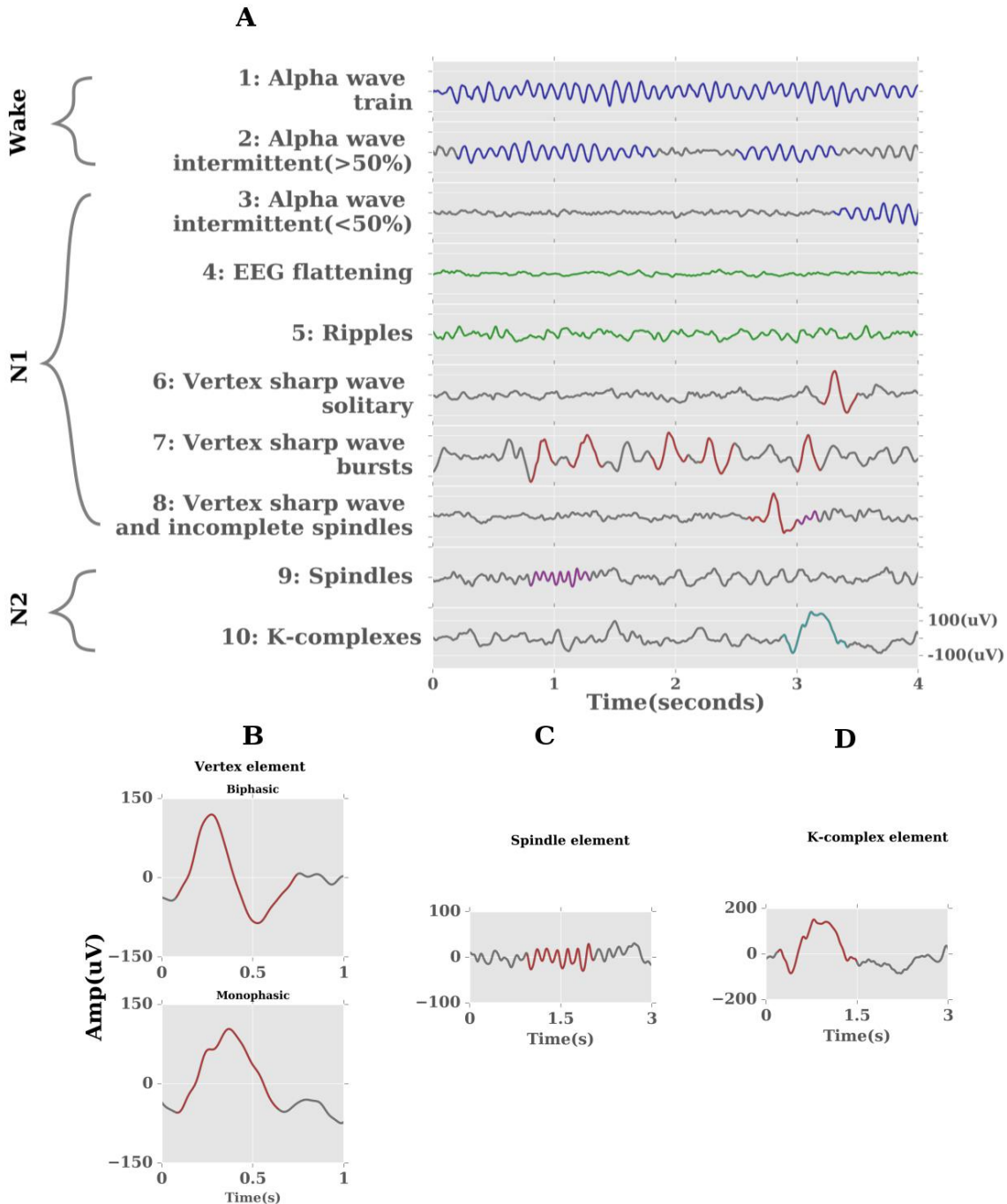
196 Hori 8: Contains at least one vertex wave and an incomplete spindle (<0.5 sec).

197 Hori 9: Contains one well defined spindle (>0.5 sec).

198 **K-complexes:**

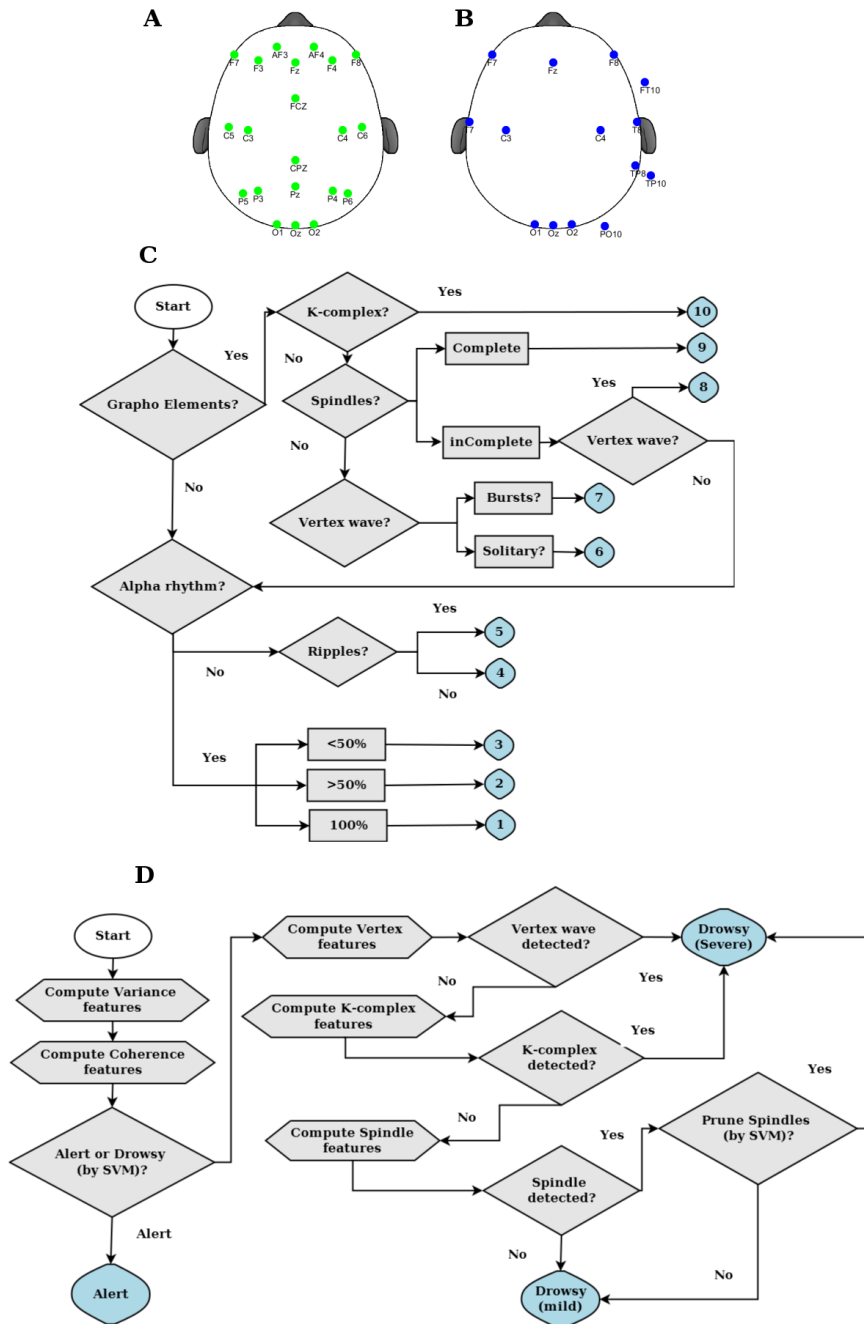
199 K-complexes are grapho elements that occur in the stage N2 of sleep (modified Hori 10). It
200 starts with a sharp positive wave followed by a large negative wave. The duration of the initial
201 negative wave should be smaller than the positive wave. The overall duration of the K-complex
202 must be at least 0.5 sec.

203 Hori 10: Contains at least one well defined K-complex.



204

205 *Fig 2: (A) Modified Hori scale for detecting differing alertness levels using EEG. The grey waves*
 206 *indicate background activity and coloured regions indicate characteristic elements for respective*
 207 *Hori stages. AASM based sleep stage classification is also represented for compatibility to classical*
 208 *sleep scoring. Grapho-elements of Hori scale in detail: (B) Vertex sharp waves: Biphasic consists of*
 209 *a sharp negative deflection followed by a positive one, whereas Monophasic consists of only a*
 210 *sharp negative deflection. (C) Spindles: transient patterns with frequency (12-16 Hz) and*
 211 *minimum duration of 0.5 sec. (D) K-complex elements: sharp positive deflection followed by a*
 212 *larger negative one with a duration of at least 0.5 sec.*



213

214 *Fig 3: (A) Electrode sites used for manual Hori scoring based on 21 channels of the locations*
 215 *mainly derived from 10-20 electrode sites. (B) Electrodes used for automatic algorithmic method*
 216 *based on sampling from locations in Occipital, Central, Temporal, Parietal, Frontal regions. (C)*
 217 *Step by step technique to manually score each trial using the Hori scale. The preliminary step*
 218 *involves identifying presence of grapho-elements followed by specific identification of k-complexes,*
 219 *spindles and vertex waves. In the absence of grapho-elements, the trials are scored with*
 220 *identification of alpha rhythms. (D) Brief flow chart of the automatic algorithm. The preliminary*
 221 *step involves computation of the predictor variance and coherence features, followed by*
 222 *identification of alert and drowsy trials using SVM. Further, drowsy trials are identified into*
 223 *specific grapho-elements using detectors of elements like vertex, k-complex, spindles.*

224 **2.5. Manual Hori-scoring**

225 For the purpose of manually scoring each epoch according to the Hori scale, the EEG data was
226 further low pass filtered below 20 Hz and only 21 channels (Fig. 3(A)) derived using the
227 standard 10-20 system were evaluated. The details of manual scoring is as follows:

228 Dataset#1: Each pre trial epoch (-4000 to 0ms) was rated independently by 3 raters. Of which
229 one was an experienced electrophysiologist (rater C) and 2 of the other raters (A, B) had learnt
230 the technique immediately prior to scoring them independently. All participants were scored
231 by the 3 raters, except for one participant that was scored only by raters A and B. As data from
232 all participants was used based on consensus rule developed in section 2.6.1 this did not affect
233 the results in anyway.

234 Dataset#2: Each pre trial epoch (-4000 to 0ms) was rated independently by 1 rater and was
235 further verified with another experienced rater. One participant was ignored from further
236 analysis as the original trial order could not be recovered from the raw EEG data.

237 The raters in dataset#1 scored each trial based on a manual algorithm depicted in Fig 3(C). The
238 rater in dataset#2 scored each trial based on the description provided in (Ogilvie, 2001).

239 **2.6. Automatic method**

240 The automatic algorithm was first developed and tested using Dataset#1 and then
241 independently validated using Dataset#2.

242 **2.6.1. Group consensus rule: creation of gold standard dataset**

243 Before training and testing the algorithm, we decided to create labels in our input data
244 (Dataset#1) that can be used by our algorithm for supervised learning. In our case, we decided
245 to create a gold standard label for each trial that is based on a group consensus rule. For this
246 purpose, we first subdivided the Hori ratings of each epoch per rater into Alert (Hori: 1,2),
247 Drowsy-mild(Hori: 3,4,5), Drowsy-severe(Hori: 6,7,8,9,10). The gold standard label was
248 computed using a simple majority among the raters. If there was no consensus, then the
249 corresponding trials were ignored from further analysis. This group consensus rule was used in
250 Dataset#1 and each trial was labelled into Alert, Drowsy (mild), Drowsy (severe). The creation
251 of this gold standard dataset ensured that the algorithm was trained and tested with trials that
252 were unambiguous and non-spurious.

253 **2.6.2. Electrode Choices**

254 The electrodes depicted in Fig 3(B) were chosen for computing the various features used in
255 different steps of the algorithm. The electrodes were chosen in such a way that we sample the
256 Occipital, Frontal, Central, Parietal, Temporal regions. Furthermore, the choices were motivated
257 for maximising the signal to noise ratio for the given reference electrode (Cz).

258 Dataset#1: Occipital: Oz, O1, O2; Frontal = F7, F8, Fz; Central = C3, C4;
259 Parietal = Pz; Temporal = T7, T8, TP8, FT10, TP10;

260 Dataset#2: Occipital: E75, E70, E83; Frontal = E27, E123, E11; Central = E35,
261 E110; Parietal = E90; Temporal = E109, E101, E115, E100;

262 A brief flow chart of the automatic algorithm is shown in Fig 3(D).

263 2.6.3. Support Vector Machines

264 The first step in our algorithm involves computing features that are capable of distinguishing
265 the various levels of alertness in the data. After which the features are used to devise a classifier
266 capable of separating the Alert (Hori:1-2) from Drowsy (Hori: 3-10). We decided to use Support
267 vector machines for this part of the classification as the classification problem is guaranteed to
268 converge to an optimal solution (Platt, 1998; Tagliazucchi et al., 2012).

269 Support vector machines (SVM) are a class of supervised learning models. Formally, SVM
270 consists of building a hyperplane or a set of hyperplanes in a high dimensional space with the
271 criteria to maximise the distance of separation between the closest data (train-data) point of
272 any class (functional margin) (Cortes and Vapnik, 1995). The choice of such a functional margin
273 would lower the generalization error for new data points (test-data). The motivation to map the
274 data onto higher dimensional space is driven by the fact that most often the classes are
275 inseparable in the lower dimensional space (Boser et al., 1992). The mapping to higher
276 dimensional space is achieved by the use of a kernel function $k(x, y)$.

277 The kernel function avoids the need to compute individual data points in the transformed data
278 space (computationally expensive) by using the euclidean inner product (kernel trick). In our
279 paper, we used the MATLAB interface of the open source machine learning library (LIBSVM)
280 (Chang and Lin, 2011) that supports use of kernel SVMs for nonlinear mappings. We used the
281 Radial Basis Function (RBF) as our kernel $k(x, y) = e^{(-\gamma||x-y||^2)}$.

282 For training the classifier to produce optimal performance (accuracy) we need to select the
283 optimal value of (γ, C) . γ controls the curvature of the hyperplane and C represents the penalty
284 parameter for the soft-margin. Parameter selection is achieved by performing a grid search in
285 (γ, C) in the space $2^{-1}, \dots, 2^{25}$. We could not perform a leave one participant out cross
286 validation, as this would produce an overfitting of parameters as different people fell asleep in
287 different ways (proportion of alert, drowsy(mild), drowsy(severe) trials). Hence the data from
288 all participants was collated and then divided into 5-folds (Tagliazucchi et al., 2012). Each of the
289 5-folds was made using stratified sampling such that the overall representation of sub-classes
290 remained similar in each fold. This will avoid the problems of over-representation prevalent
291 while using random-sampling. The first four folds were used to train the classifier to choose the
292 parameters (γ, C) and the last fold was used to test the same. In order to measure the
293 performance of the classifier we decided to use sensitivity, specificity, f1- score.

294 The definition of the performance measures used are as follows:

295 Accuracy: This is defined as the number of correctly classified data points divided by the overall
296 number of classifications made.

297 Sensitivity: This refers to the ability of a classifier to correctly detect the true class among the
298 classifications made. It is obtained by the $(TP/TP+FN)$. It is also known as recall. TP: True
299 Positives, FN: False Negatives.

300 Specificity: This refers to the ability of a classifier to correctly ignore the class that don't belong
301 to the true condition. It is obtained by $(TN/TN+FP)$. TN: True Negatives, FP: False Positives.

302 F1-score: This is the harmonic mean between precision and recall. Precision refers to measure
303 of exactness of classifier. It is obtained by $(TP/TP+FP)$. TN: True Positives, FP: False Positives.
304 Recall refers to the sensitivity of the classifier.

305 As the input data contains different kinds of features, it was scaled using the minimum value
306 and range before applying the SVM.

307 2.6.4. Feature Computation

308 To use the above mentioned SVM for classification we need to compute the following features
309 that can allow the classifier to distinguish between different classes.

310 Predictor Variance:

311 The EEG data in occipital region was first decomposed into time-frequency for each spatial
312 sample (electrode) per epoch (-4000 to 0ms pre-trial). Predictors for each epoch were then
313 generated based on the variations in the spectral power of the frequency bins A:[2-4 Hz],B:[8-10
314 Hz],C:[10-12 Hz],D:[2-6 Hz] per epoch. The predictors were then fit to the data per electrode-
315 epoch and the variance explained is computed per electrode-epoch.

316 The first step is to transform the data $x[n]$ into time-frequency representation (predictors)
317 using the below formula, where n represents time domain with $1 \leq k \leq N$

$$318 \quad X(k) = \sum_{n=1}^N x(n) e^{\frac{-j2\pi(k-1)(n-1)}{N}}$$

319 The next step is to compute the power in the transformed representation

$$320 \quad Power = X(k).X^*(k)$$

321 Followed by computing the predictor variance

$$322 \quad PredictorVariance_i = 100 - 100 * \frac{Var(Power-X(k_i))}{Var(X(k_i))}$$

323 Where i represents the frequency band index (A,B,C,D) and Var represents the residual
324 variance. Intuitively the predictor variance tries to capture the variance in the signal explained
325 by different frequency bands and the SVM later on uses this feature for classification.

326 Coherence:

327 Coherence was computed per trial in the electrodes in the occipital, frontal, central, temporal
328 regions in the frequency bins: Delta:[1-4 Hz], Theta:[4-7 Hz], Alpha:[7-12 Hz], Sigma:[12-16 Hz],
329 Gamma:[16-30 Hz]

$$330 \quad C(t, f) = \frac{|S_{ij}(t, f)|^2}{S_{ii}(t, f).S_{jj}(t, f)}$$

331 Where $C(t, f)$ represents the coherence value at trial t and frequency band f

332 S_{ij} represents cross power spectral density between signal i and j

333 S_{ii}, S_{jj} represents auto power spectral density.

334 After the detection of the drowsy trials using the above mentioned features, the following
335 detectors are used to further subclassify them into drowsy (mild) and drowsy (severe).

336

337

338

339 **2.6.5. Grapho element detectors**

340 **2.6.5.1. Vertex-wave-detectors**

341 Both monophasic and biphasic waves were detected using the parietal electrodes. The signal
342 was first resampled to 100 Hz and then filtered from 0.25 -6 Hz. After which the signal in each
343 trial was further scaled with respect to its minima. Peaks that are above a specific threshold are
344 then detected and the negative peaks are used to classify the elements as mono or biphasic
345 (algorithmic, parametric details described in supplementary methods)

346 **2.6.5.2. Spindle detectors**

347 Spindles were detected using the temporal electrodes. The signal was first resampled to 100 Hz
348 and then a continuous wavelet transform using morlet function as the mother wavelet was
349 applied. The coefficients of this transform are then normalized and then further provided a rank
350 according to the magnitude. Each rank is further normalized to compute the probability of the
351 spindle occurrence at each time point. Further spindle locations are pruned using a snapshot of
352 the detected location (algorithmic, parametric details described in supplementary material).

353 **2.6.5.3. K-complex detectors**

354 K-complexes were detected using all the electrode sites in Fig 3(B). The signal was first
355 resampled to 100 Hz and then filtered from 0.25-6 Hz. After which the signal in each trial was
356 further scaled with respect to its maxima. Peaks that are separated by at least 1.5 sec and below
357 a specific threshold are then detected. Further to which peaks above a specific threshold in the
358 next 1.5 sec are detected. The positive peak should be at least half of the magnitude of the
359 negative (algorithmic, parametric details described in supplementary material).

360 In summary a total of 32 features (12 from predictor variance; 20 from coherence) are used in
361 the first stage detection of alert trials from drowsy trials. After the drowsy trials are parsed by
362 the element detectors, the spindle elements are pruned again by a separate SVM using the same
363 32 features as above (depicted in Figure 3(D)).

364

365

366

367

368

369

370

371

372

373

374 **3. Results**

375 **3.1. Manual Hori-scoring**

376 In order to measure the reliability of scores given by the 3 different raters on different subjects
377 in Dataset#1 we used two different measures of inter-rater agreement (Fig 4).

378 Firstly, we used Krippendorff's alpha to compute the agreement between the 3 raters (A, B, C)
379 per subject of Dataset#1. In general alpha scores of above 0.8 are reliable and those between
380 0.8 and 0.667 can only be used to draw tentative conclusions (Giannantonio, 2010). We can
381 observe from Fig 4(A) at least 9 subjects are below 0.667 (with mean being 0.65) indicating the
382 unreliable nature of scoring each subject among raters. Secondly, we used Cohen's kappa score
383 (weighted) to measure the degree of inter-rater agreement between pairs of raters (AB, AC, BC)
384 of Dataset#1. In general kappa values of above 0.8 are considered strong, between 0.8 and 0.4 as
385 strong to weak, below 0.4 as poor (McHugh, 2012). We can observe from Fig 4(B) at least 12
386 subjects are below 0.4 in the various scorer pairs indicating the unreliable nature of scoring per
387 subject among raters.

388 In particular the degree of disagreement was high for subjects that didn't have a dominant
389 alpha, thereby affecting the ability to rate the Hori scores as (1,2,3). For other subjects the
390 degree of disagreement mainly rose due to the mislabelling of graphical elements. Examples of
391 such typical cases of grapho elements are shown in Fig 4(C, D, E).

392 **3.2. Automatic method**

393 **3.2.1. External Validation: Spindle, K-complex detectors**

394 The Spindle, K-complex detectors were validated externally using the DREAMS database along
395 with other state of the art algorithms (Devuyst et al., 2011, 2010; Tsanas and Clifford, 2015)
396 (detailed validation method in supplementary material). The validation results are shown in Fig
397 5. This validation ensured the element detectors perform on par with the state of the art
398 methods. The parameters used in spindle, k-complex detectors (like spindle duration, k-
399 complex amplitude etc.) were fixed with respect to the external databases and the same
400 parameters were used in the validation of both Dataset #1, #2.

401 **3.2.2. Validation: Dataset#1**

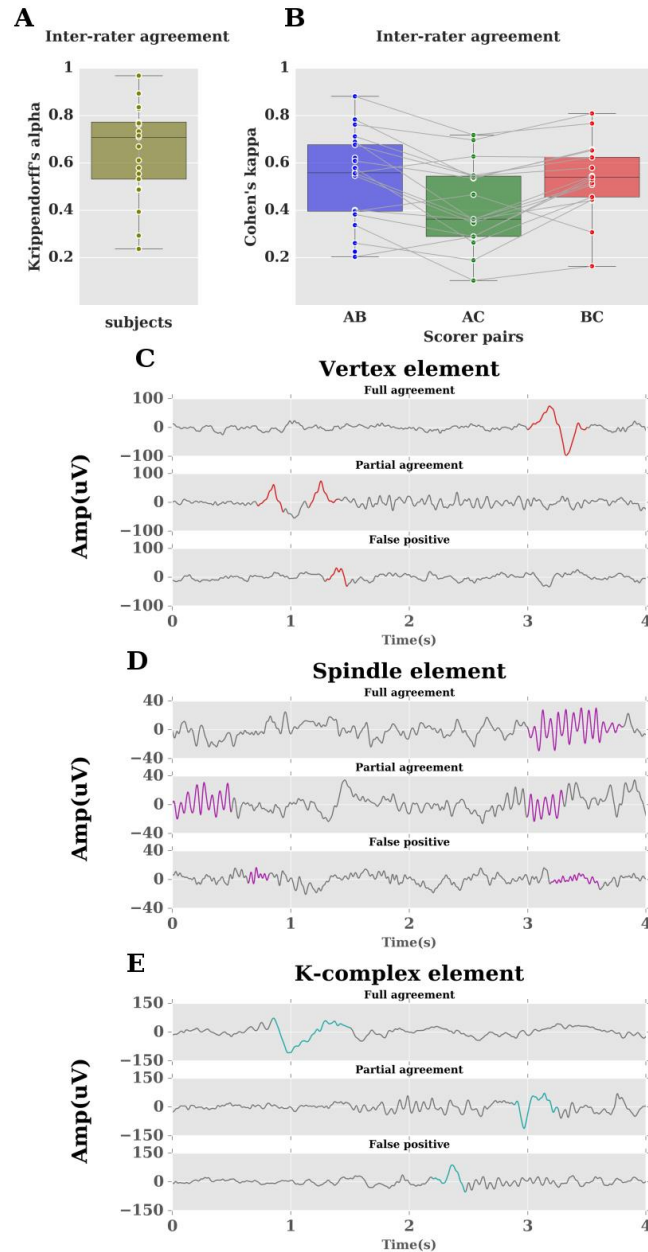
402 After the group consensus rule (sec 2.6.1) was applied on Dataset#1, the number of trials in the
403 gold standard dataset in each class were: Alert:475, Drowsy(mild):1104, Drowsy(severe):281.
404 Around 1306 trials (40%) did not have a consensus rating and hence were ignored from further
405 analyses. This shows that about 40% of the overall trials didn't have any consensus among the 3
406 different raters, further adding evidence to the disagreement among scorers mentioned in
407 section 3.1.

408 Trials from all participants in Dataset#1 were first collated and then partitioned into 5 folds.
409 The partition was made using stratified sampling such that the overall representation of sub-
410 classes remained similar in each fold. The training set further constituted of the first 4 folds and
411 the test set consisted of the 5th fold. This procedure was repeated for 5 times as described in
412 Fig 6(A). For each iteration the performance measures like sensitivity, specificity, f-1 scores
413 were generated and the results are shown in Fig 7(A, B, C).

414 **3.2.3. Independent validation: Dataset#2**

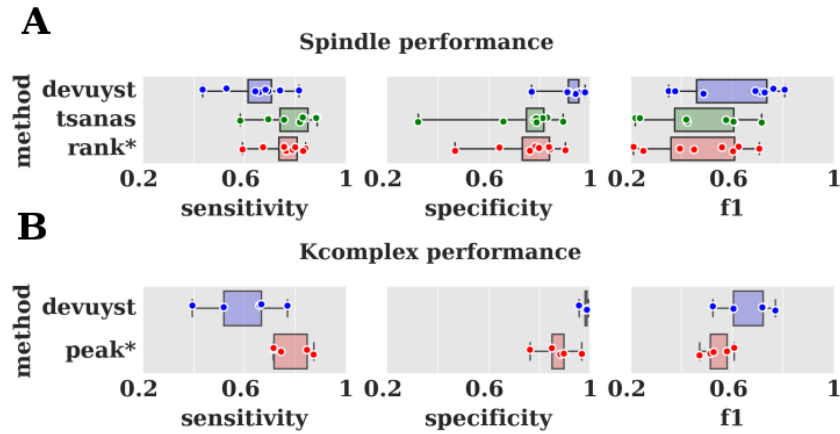
415 We decided to validate the algorithm (trained using dataset#1) on an independent dataset#2 to
416 test its generalisability. This would mean that the hyper parameters (γ, C), support vectors
417 trained using dataset#1 were directly applied on the dataset #2 without retraining. The
418 number of trials in dataset#2 in each class were: Alert: 6049, Drowsy(mild): 7200,
419 Drowsy(severe): 475. The dataset was divided into 5 folds using stratified sampling as before.
420 The set#1 consisted of the first 4 folds and the set#2 consisted of the 5th fold. Thus set#1
421 contained atleast 4 times the number of trials in set#2 and hence similar in composition to the
422 train and test sets in dataset #1 where train had at least 4 times the number of trials in test set.
423 The same procedure was repeated for 5 times as described in Fig 6(B). For each iteration the
424 performance measures like sensitivity, specificity, f-1 scores were generated and the results are
425 shown in Fig 7(D, E, F).

426 The above mentioned methods in Dataset#2 tend to validate the automatic method against the
427 human scorer. However, to claim that the automatic method out performs the human scorer in
428 Dataset#2, we decided to further validate the same against an independent measure of
429 drowsiness. Coefficient of variation (CoV) in reaction times has been used previously to
430 measure drowsiness and is independent of both the observer and the algorithm's pre-trial
431 information (Bareham et al., 2014). We separated the trials among different classes of
432 drowsiness using both the automatic and manual method. Further, CoVs were computed per
433 participant for all classes (generated both by automatic and manual method) that contained at
434 least 10 trials. Repeated measures ANOVAs on classes from automatic method yielded a main
435 effect of drowsiness on CoV with $F(2,22) = 9.25, p < 0.01$. Post-hoc tests (multiple comparisons
436 corrected with bonferroni) yielded differences between mild and severe drowsiness (Cohen's d:
437 -0.95, $p < 0.05$), alert and severe drowsiness (Cohen's d: -0.91, $p < 0.05$). However, the manual
438 method failed to produce any main effect of drowsiness on CoV with $F(2,8) = 1.2$ with $p > 0.05$.
439 These measures shown in Fig 7(G), clearly indicate the utility of the automatic method over
440 manual scoring.



441

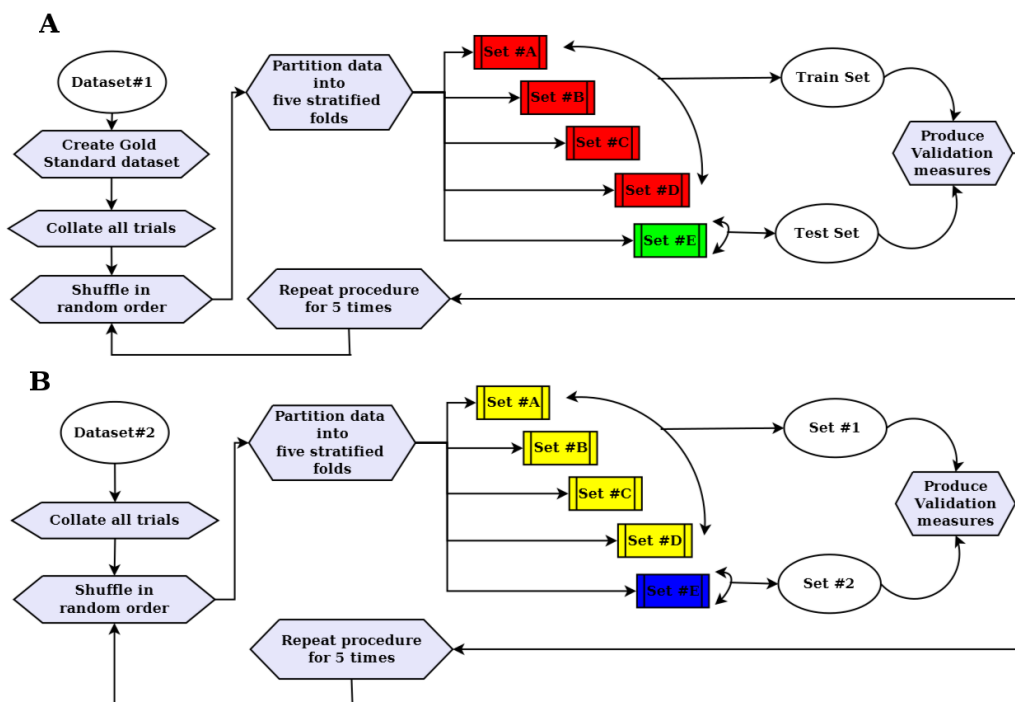
442 *Fig 4: Inter-rater agreement among different scorers (A,B,C). (A) depicts agreement measured*
443 *using Krippendorff's alpha. Each data point refers to score from a single subject. (B) depicts*
444 *agreement measured using Cohen's kappa. Each data point refers to kappa scores from a single*
445 *subject based on a pair of two different scorers. Inter-rater disagreement is typically caused due to*
446 *misclassification of Grapho elements: (C) depicts typical Vertex wave agreement/disagreement*
447 *among scorers highlighted in red. (D) depicts typical Spindle element agreement/disagreement*
448 *among scorers highlighted in magenta. (E) depicts typical K-complex agreement/disagreement*
449 *among scorers highlighted in cyan. Full agreement refers to cases where all 3 raters agree, Partial*
450 *agreement refers to cases where 2 of them agree, and false positives refer to cases where at least*
451 *one of the rater misclassifies an element.*



452

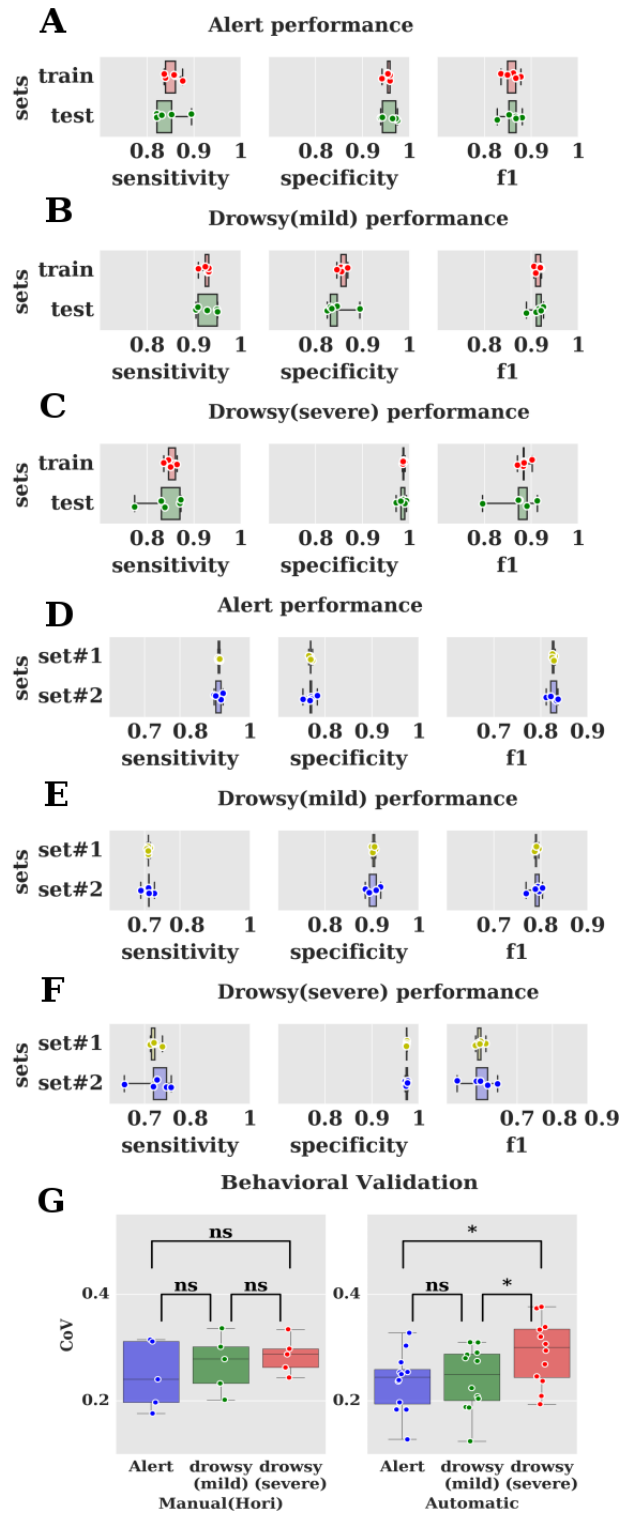
453 *Fig 5: Performance validation of grapho-element detectors with online database (DREAMS). The*
 454 *spindle detector was validated with state of the art algorithms from (Devuyst et al., 2011; Tsanas*
 455 *and Clifford, 2015). The rank* algorithm developed in this paper performs comparable to the*
 456 *above mentioned algorithms. The K-complex detector was validated with state of the art*
 457 *algorithms from (Devuyst et al., 2010). The peak* algorithm developed in this paper performs*
 458 *comparable to the above mentioned algorithms.*

459



460

461 *Fig 6: Curation of test and train datasets. (A) depicts creation of test and train dataset using*
 462 *Dataset #1 by five-fold stratified partition and this procedure is repeated for 5 times to produce*
 463 *validation measures. (B) depicts creation of Set #1, Set#2 using Dataset #2 by five-fold stratified*
 464 *partition and Set#1 is created by merging the first four sets and fifth set is constituted as Set #2*
 465 *and this procedure is repeated for 5 times to produce validation measures.*



466

467 *Fig 7: Validation measures of automatic algorithm. Validated with Dataset#1 using steps*
 468 *described in Fig 6(A). Results are depicted in the figure (A,B,C). The automatic algorithm was*
 469 *validated in an independent manner using Dataset#2 using steps described in Fig 6(B). Results are*
 470 *depicted in the figure (D,E,F). Validation with an independent measure (Coefficient of variation in*
 471 *reaction times) shows the algorithm reliably detecting differences (using repeated measures*
 472 *ANOVA) better than the manual scoring in figure G. ns: denotes $p > 0.05$, * denotes $p < 0.01$*
 473 *(bonferroni corrected)*

474 **4. Discussions and Conclusions**

475 In this paper, we have first described the pervasive problem of varying levels of alertness during
476 cognitive experiments, particularly during eyes closed experiments. Such a scenario is further
477 exacerbated in resting state EEG recordings. In many cases data from such experiments are used
478 to compute measures like connectivity etc. that may further be contaminated by participants
479 falling asleep (Tagliazucchi et al., 2012). This situation potentially contributes to wider
480 problems faced by the scientific community such as the replication crisis.

481 In the past the problem of extreme relaxation and drowsiness has been ignored sometimes by
482 cognitive scientists, and only taking into account by looking at reaction times and removing the
483 sections where the participant was not responding or was too slow. Apart from visible changes
484 in reaction times, there are changes in important processes like attention and perception as the
485 participant drifts across varying levels of alertness (Goupil and Bekinschtein, 2012). Hence it is
486 of paramount importance to control for varying levels of alertness. We have tried to solve this
487 problem in an objective manner as follows. We first described the use of Hori scale that has
488 been validated previously to detect the levels of alertness during sleep onset process. However
489 the Hori scoring with 4 sec epochs is impractical to perform as it is highly subjective and time
490 consuming (Ogilvie, 2001). Using 3 independent raters on Dataset#1 we further quantified the
491 inter-rater agreement using Krippendorff's alpha and Cohen's kappa metrics to show low levels
492 of agreement among the raters. This motivated us to develop an algorithmic solution that can be
493 used to measure the level of alertness in a reliable manner.

494 There have been attempts in the past to detect varying level of alertness using algorithms.
495 However, they suffer from several disadvantages. Firstly, such rule based algorithms (Olbrich et
496 al., 2009) have validated their system using physiological measures like heart-rate variability
497 etc. This further adds a layer of confound as measures of alertness needs to be related again
498 with physiological measures. Secondly, other set of algorithms (Crisler et al., 2008;
499 Gudmundsson et al., 2005; Tagliazucchi et al., 2012) have been developed using traditional
500 sleep stage based scoring. Such systems suffer from lack of resolution as they are validated with
501 sleep scoring techniques that use 30 sec epochs. Thus they are unsuitable to match the micro
502 dynamics in alertness observed during cognitive tasks. To our knowledge this is the first time an
503 algorithmic solution has been attempted to measure the varying level of alertness and
504 simultaneously verifying the same using a previously well validated system like Hori.

505 In the current work we have shown that predictor variance, coherence and grapho element
506 detectors allow us to micro measure the level of alertness. We have constructed a classifier
507 based on SVM and individual element detectors and have achieved sensitivity, specificity, f1-
508 score of more than 0.8 in all subclasses (alert, drowsy(mild), drowsy(severe)) with respect to
509 manual Hori scoring (gold standard from different raters). We have also validated our algorithm
510 with a second independent dataset using different task conditions and recording electrode sites
511 (using the same hyper parameters and support vectors trained using the first dataset). This
512 produced a sensitivity, specificity, f1-score of more than 0.7 in all subclasses. The main reason
513 the performance reduces for drowsy(severe) subclass in dataset#2 is due to lack of gold
514 standard comparison and fewer number of trials in this category. As the dataset#2 is scored
515 only by one person it is prone to error (in a fashion similar to dataset#1 as depicted by varying
516 levels of interrater agreement in Fig 4). This motivated us to show that our algorithm
517 outperforms the manual scorer. Hence we employed a previously established independent
518 behavioural measure of drowsiness using Coefficient of variation in reaction times. We further
519 showed that the automatic algorithm captures the variations in CoV better than the manual

520 scorer in Fig 7(G). This stands testament to the generalisability of our method in detecting
521 alertness levels across new datasets.

522 However the usage of Hori scale as validator has some disadvantages. Firstly, it is difficult to
523 detect Hori stages (1-3) on participants who lack prominent alpha waves (Ogilvie, 2001). This
524 would make these participants difficult to score manually, thereby explaining the lower
525 sensitivity of the algorithm in Drowsy (mild) subclass compared to the other classes. However,
526 this is a problem for the human scorer, as the automatic algorithm is relatively immune to this
527 problem. As it operates on relative variances across different bands rather than raw amplitude.
528 Secondly, it has also been reported that the Hori stage (4) also doesn't last long and hence is
529 difficult to score (Ogilvie, 2001). Such samples would have had a high level of disagreement
530 among scorers and hence would have been ignored while computing the gold standard dataset.
531 Consequently, the difficult trials would not have been used for training the algorithm and hence
532 it may not be able to detect any such trials in a new dataset. Thirdly, one of the main reasons for
533 validating the algorithm with 3 subclasses is mainly due to lack of consensus in individual
534 grapho elements. In order to truly validate the grapho elements we would need a dataset rich in
535 those elements and also scorers who are able to consistently detect the grapho elements in a
536 correct fashion.

537 The automatic algorithm devised here could be improved in several ways. Firstly, the current
538 algorithm uses SVM with RBF kernels, other kernels choices like polynomial functions could be
539 evaluated for making the optimal choice. Secondly, we performed only basic preprocessing of
540 the pre trial data. However it is well known that artifacts like eye movement, sweating, muscle
541 artifacts can contribute to noise in the data. Hence the performance of the algorithm would
542 improve if noise reduction measures are employed. However, we didn't employ such measures
543 as they are not standardized and we wanted to establish that the performance of algorithm is
544 robust under all conditions and hence performing specific pre-processing steps should not be an
545 impediment for users of our method. Thirdly, we could also try to reduce the duration of epochs
546 considered for labeling for e.g. we can check the classification accuracies of signal durations of 1,
547 2, 3 secs etc. However, validating the same would be difficult as we also need to redo the human
548 scoring with the corresponding reduced length of epochs. Fourthly, the automatic algorithm has
549 been developed only for eyes closed condition. But many cognitive experiments have eyes open
550 conditions and participants are also known to fall asleep under such active paradigms. The
551 algorithm could be adapted for such paradigms; however detailed validation needs to be
552 performed with other parallel measures of drowsiness like eye-tracking (as the Hori scale has
553 not been validated for such purposes). Fifthly, the algorithm could further be refined to produce
554 stages analogous to individual Hori stages. This would be helpful for researchers studying the
555 sleep onset process in an objective manner as many complex non-linear changes in behaviour
556 are known to occur in individual Hori stages (Noreika et al., 2017b). Finally, for quick paced
557 experiments (short pre-trial periods), the parameters for detecting certain graphoelements
558 (vertexes, k-complexes) are flexible to account for the shorter duration of the signal.

559 The applications of the algorithm include the following. Firstly, pre-trial data can be computed
560 from task data (cognitive experiments) and the non-alert trials can be removed thus controlling
561 for the effects of change in alertness levels. Secondly, we can detect and remove non-alert
562 periods of data from resting state EEG experiments in a reliable manner. Thirdly, we can
563 measure alertness as an independent variable and measure its effect on measures of interest.
564 Fourthly, the method circumvents the subjective nature of the manual Hori scoring and thus
565 enables to study the transition to sleep in an objective way. One of the most interesting aspects
566 is the generalisability of the SVM classifier and other element detectors to the independent
567 dataset#2, showing the high degree of transferability of this method, without having to retrain

568 the classifier. Fifthly, when combined with online stimulus delivery techniques, the ability of our
569 method to detect grapho elements (vertex, spindles, k-complexes) also allows us to investigate
570 the effects of these elements on the cognitive processes, for example by modulating the stimulus
571 delivery according to the occurrence of these elements. Finally, sleep researchers can use this
572 method for detecting N1 periods in the beginning of the night as well as awakenings and N1
573 periods during the full night period; further, they can also validate the detection of N2 periods
574 by using the appearance of specific graphoelements (spindles, k-complexes).

575 All of the above mentioned facets make our method a unique solution that can be used to micro
576 measure the varying alertness levels and thereby providing a valuable contribution to the study
577 of both cognitive and resting state EEG experiments at large.

578

579 **Acknowledgements**

580 This research was funded by Gates Cambridge Scholarship awarded to SRJ and Wellcome Trust
581 Biomedical Research Fellowship WT093811MA awarded to TAB. We thank Louise Goupil for
582 acquiring Dataset#1. We thank Valdas Noreika for providing Dataset#2 and many insightful
583 comments on the manuscript. Carmen Soria for her work on a different manuscript on manual
584 Hori scoring. We thank Srivas Chennu for his comments on a later version of the manuscript.

585 **Conflict of Interest**

586 None

587 **Author Contributions**

588 Conceptualization: SRJ, TAB

589 Data Curation: SRJ, TAB

590 Formal Analysis: SRJ, BJ, AEN, OVP, TAB

591 Funding Acquisition: TAB

592 Methodology: SRJ

593 Project Administration: TAB

594 Resources: TAB

595 Software: SRJ

596 Supervision: TAB

597 Validation: SRJ, CAB, BJ, AEN

598 Visualization: SRJ

599 Writing – original draft: SRJ

600 Writing – review & editing: SRJ, CAB, BJ, AEN, TAB

601 **5. References**

- 602 Bareham, C.A., Manly, T., Pustovaya, O. V., Scott, S.K., Bekinschtein, T.A., 2014. Losing the left side
603 of the world: Rightward shift in human spatial attention with sleep onset. *Sci. Rep.* 4, 1–5.
604 doi:10.1038/srep05092
- 605 Barry, R.J., Clarke, A.R., Johnstone, S.J., Magee, C.A., Rushby, J.A., 2007. EEG Differences Between
606 Eyes-Closed and Eyes-Closed Resting Conditions. *Int. J. Psychophysiol.* 118, 2765–2773.
607 doi:<https://doi.org/10.1016/j.clinph.2007.07.028>
- 608 Berry, R.B., Budhiraja, R., Gottlieb, D.J., Gozal, D., Iber, C., Kapur, V.K., Marcus, C.L., Mehra, R.,
609 Parthasarathy, S., Quan, S.F., Redline, S., Strohl, K.P., Ward, S.L.D., Tangredi, M.M., 2012.
610 Rules for scoring respiratory events in sleep: Update of the 2007 AASM manual for the
611 scoring of sleep and associated events. *J. Clin. Sleep Med.* doi:10.5664/jcsm.2172
- 612 Boser, B.E., Guyon, I.M., Vapnik, V.N., 1992. A Training Algorithm for Optimal Margin Classifiers,
613 in: *Proceedings of the Fifth Annual Workshop on Computational Learning Theory, COLT*
614 '92. ACM, New York, NY, USA, pp. 144–152. doi:10.1145/130385.130401
- 615 Chang, C.-C., Lin, C.-J., 2011. LIBSVM: A Library for Support Vector Machines. *ACM Trans. Intell.*
616 *Syst. Technol.* 2, 27:1--27:27. doi:10.1145/1961189.1961199
- 617 Chennu, S., Bekinschtein, T.A., 2012. Arousal modulates auditory attention and awareness:
618 Insights from sleep, sedation, and disorders of consciousness. *Front. Psychol.* 3, 1–9.
619 doi:10.3389/fpsyg.2012.00065
- 620 Cortes, C., Vapnik, V., 1995. Support-Vector Networks. *Mach. Learn.* 20, 273–297.
621 doi:10.1023/A:1022627411411
- 622 Crisler, S., Morrissey, M.J., Anch, A.M., Barnett, D.W., 2008. Sleep-stage scoring in the rat using a
623 support vector machine. *J. Neurosci. Methods* 168, 524–534.
624 doi:<https://doi.org/10.1016/j.jneumeth.2007.10.027>
- 625 Delorme, A., Makeig, S., 2004. EEGLAB: an open source toolbox for analysis of single-trial EEG
626 dynamics including independent component analysis. *J. Neurosci. Methods* 134, 9–21.
627 doi:<https://doi.org/10.1016/j.jneumeth.2003.10.009>
- 628 Devuyst, S., Dutoit, T., Stenuit, P., Kerkhofs, M., 2011. Automatic sleep spindles detection--
629 overview and development of a standard proposal assessment method. *Conf. Proc. IEEE*
630 *Eng. Med. Biol. Soc.* 2011, 1713–6. doi:10.1109/IEMBS.2011.6090491
- 631 Devuyst, S., Dutoit, T., Stenuit, P., Kerkhofs, M., 2010. Automatic K-complexes detection in sleep
632 EEG recordings using likelihood thresholds. 2010 *Annu. Int. Conf. IEEE Eng. Med. Biol. Soc.*
633 *EMBC'10* 4658–4661. doi:10.1109/IEMBS.2010.5626447
- 634 Dobler, V.B., Anker, S., Gilmore, J., Robertson, I.H., Atkinson, J., Manly, T., 2005. Asymmetric
635 deterioration of spatial awareness with diminishing levels of alertness in normal children
636 and children with ADHD. *J. Child Psychol. Psychiatry* 46, 1230–1248. doi:10.1111/j.1469-
637 7610.2005.00421.x
- 638 Giannantonio, C.M., 2010. Book Review: Krippendorff, K. (2004). *Content Analysis: An*
639 *Introduction to Its Methodology* (2nd ed.). Thousand Oaks, CA: Sage. *Organ. Res. Methods*
640 13, 392–394. doi:10.1177/1094428108324513
- 641 Goupil, L., Bekinschtein, T. a., 2012. Cognitive processing during the transition to sleep. *Arch.*
642 *Ital. Biol.* 150, 140–154. doi:10.4449/aib.v150i2.1247
- 643 Gudmundsson, S., Runarsson, T.P., Sigurdsson, S., 2005. Automatic Sleep Staging using Support
644 Vector Machines with Posterior Probability Estimates. *Int. Conf. Comput. Intell. Model.*

- 645 Control Autom. 2, 366–372. doi:10.1109/CIMCA.2005.1631496
- 646 Iber, C., Ancoli-Israel, S., Chesson, A.L., Quan, S., 2007. The AASM Manual for the Scoring of Sleep
647 and Associated Events: Rules, Terminology and Technical Specifications. Westchester, Am.
648 Acad. Sleep Med.
- 649 Johns, M.W., 1991. A New Method for Measuring Daytime Sleepiness: The Epworth Sleepiness
650 Scale. Sleep 14, 540–545. doi:10.1093/sleep/14.6.540
- 651 Kouider, S., Andrillon, T., Barbosa, L.S., Goupil, L., Bekinschtein, T.A., 2014. Inducing task-
652 relevant responses to speech in the sleeping brain. Curr. Biol. 24, 2208–2214.
653 doi:10.1016/j.cub.2014.08.016
- 654 Lajnef, T., Chaibi, S., Eichenlaub, J.-B., Ruby, P.M., Aguera, P.-E., Samet, M., Kachouri, A., Jerbi, K.,
655 2015. Sleep spindle and K-complex detection using tunable Q-factor wavelet transform and
656 morphological component analysis. Front. Hum. Neurosci. 9, 1–17.
657 doi:10.3389/fnhum.2015.00414
- 658 McHugh, M.L., 2012. Interrater reliability: the kappa statistic. Biochem. Medica 276–282.
659 doi:10.11613/BM.2012.031
- 660 Niedermeyer, E., Silva, F.H.L. Da, 2004. Electroencephalography: Basic Principles, Clinical
661 Applications, and Related Fields, 5th ed. ed, Lippincott Williams and Wilkins. Philadelphia ;
662 London : Lippincott Williams & Wilkins.
- 663 Noreika, V., Canales-Johnson, A., Harrison, W.J., Johnson, A., Arnatkevičiūtė, A., Koh, J., Chennu, S.,
664 Bekinschtein, T.A., 2017a. Wakefulness state modulates conscious access: Suppression of
665 auditory detection in the transition to sleep. bioRxiv 1–34.
- 666 Noreika, V., Kamke, M.R., Canales-Johnson, A., Chennu, S., Mattingley, J.B., Bekinschtein, T.A.,
667 2017b. Neurobehavioral dynamics of drowsiness. bioRxiv 1–36. doi:10.1101/155754
- 668 Ogilvie, R.D., 2001. The process of falling asleep. Sleep Med. Rev. 5, 247–270.
669 doi:10.1053/smr.2001.0145
- 670 Olbrich, S., Mulert, C., Karch, S., Trenner, M., Leicht, G., Pogarell, O., Hegerl, U., 2009. EEG-
671 vigilance and BOLD effect during simultaneous EEG/fMRI measurement. Neuroimage 45,
672 319–332. doi:10.1016/j.neuroimage.2008.11.014
- 673 Platt, J., 1998. Sequential Minimal Optimization: A Fast Algorithm for Training Support Vector
674 Machines.
- 675 Rodenbeck, A., Binder, R., Geisler, P., Danker-Hopfe, H., Lund, R., Raschke, F., Weeß, H.G., Schulz,
676 H., 2006. A review of sleep EEG patterns. Part I: A compilation of amended rules for their
677 visual recognition according to Rechtschaffen and Kales. Somnologie 10, 159–175.
678 doi:10.1111/j.1439-054X.2006.00101.x
- 679 Tagliazucchi, E., Laufs, H., 2014. Decoding Wakefulness Levels from Typical fMRI Resting-State
680 Data Reveals Reliable Drifts between Wakefulness and Sleep. Neuron 82, 695–708.
681 doi:10.1016/j.neuron.2014.03.020
- 682 Tagliazucchi, E., von Wegner, F., Morzelewski, A., Borisov, S., Jahnke, K., Laufs, H., 2012.
683 Automatic sleep staging using fMRI functional connectivity data. Neuroimage 63, 63–72.
684 doi:10.1016/j.neuroimage.2012.06.036
- 685 Tanaka, H., Hayashi, M., Hori, T., 1996. Statistical features of hypnagogic EEG measured by a new
686 scoring system. Sleep 19, 731–738.
- 687 Tsanas, A., Clifford, G.D., 2015. Stage-independent, single lead EEG sleep spindle detection using
688 the continuous wavelet transform and local weighted smoothing. Front. Hum. Neurosci. 9,

689 181. doi:10.3389/fnhum.2015.00181

690 Warby, S.C., Wendt, S.L., Welinder, P., Munk, E.G.S., Carrillo, O., Sorensen, H.B.D., Jennum, P.,
691 Peppard, P.E., Perona, P., Mignot, E., 2014. Sleep-spindle detection: crowdsourcing and
692 evaluating performance of experts, non-experts and automated methods. *Nat. Methods* 11,
693 385–92. doi:10.1038/nmeth.2855

694 **6. Supplementary methods**

695 **6.1. Vertex wave detectors**

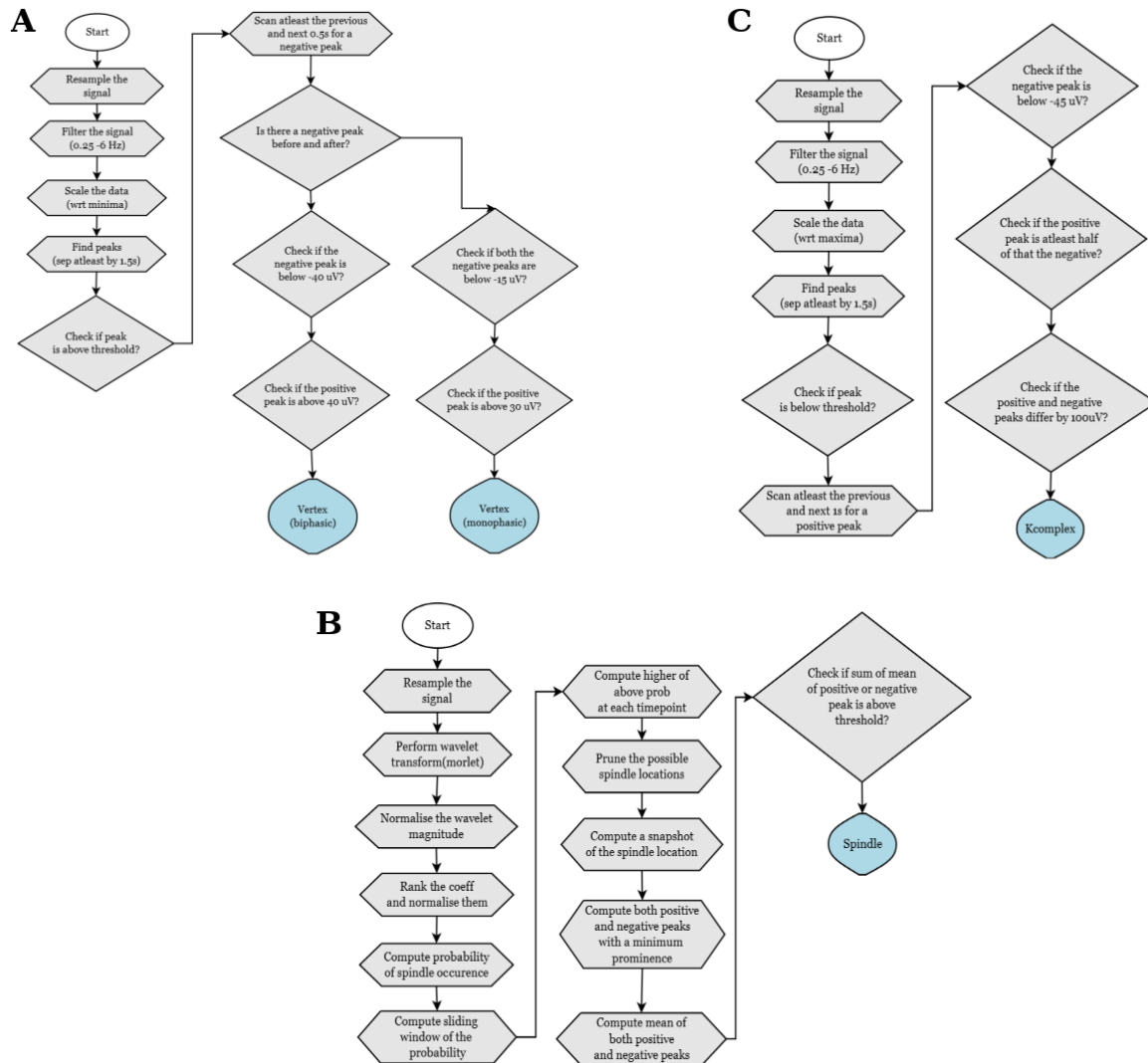
696 The two kinds of vertex waves depicted in Fig 2(B) are detected using the algorithm in Fig 8(A).
697 As there was no online database available for vertex sharp waves it was not validated
698 independently.

699 **6.2. Spindle detectors**

700 The spindles are detected using the algorithm in Fig 8(B). The algorithm was validated against
701 an online database (DREAMS) (Devuyst et al., 2011) The data in the .edf format was first
702 converted into EEGLAB format and was filtered from 0.5 - 20 Hz. The data was further
703 resampled to 100 Hz and further epoched for each 4 sec. The gold standard dataset was created
704 by merging the annotations from two experts for all the eight excerpts in the database. Our
705 spindle detection algorithm was then validated against this gold standard along with state of the
706 art methods that have already been validated against the same database (Devuyst et al., 2011;
707 Tsanas and Clifford, 2015)

708 **6.3. K-complex detectors**

709 The Kcomplexes are detected using the algorithm in Fig 8(C). The approach developed here is
710 similar (in terms of minima detection) to detectors developed elsewhere (Lajnef et al., 2015).
711 The algorithm was validated against an online database (DREAMS) (Devuyst et al., 2010). The
712 data in the .edf format was first converted into EEGLAB format and was filtered from 0.5 - 20 Hz.
713 The data was further resampled to 100 Hz and further epoched for each 4 sec. The gold
714 standard dataset was created by merging the annotations from two experts for the five excerpts
715 in the database. Our kcomplex detection algorithm was then validated against this gold standard
716 along with state of the art methods that have already been validated against the same database
717 (Devuyst et al., 2010)



718

719 *Fig 8: (A) Vertex wave detector algorithm. The preliminary step involves resampling, filtering and*
 720 *scaling of the signal to identify the peaks in the signal. Further the specific characteristics of the*
 721 *peaks are used to identify mono and biphasic vertex waves. (B) Spindle detector algorithm. The*
 722 *preliminary step involves resampling and using wavelet transform to identify the regions with high*
 723 *probability of occurrence of spindle waves. Further the specific characteristics of the waves are*
 724 *used to prune them. (C) K-complex detector algorithm. The preliminary step involves resampling,*
 725 *filtering and scaling of the signal to identify the peaks in the signal. Further the specific*
 726 *characteristics of the peaks are used to identify k-complex waves.*